ISSN 0023-1584, Kinetics and Catalysis, 2009, Vol. 50, No. 2, pp. 149–155. © Pleiades Publishing, Ltd., 2009.
Original Russian Text © Yu.K. Karasevich, 2009, published in Kinetika i Kataliz, 2009, Vol. 50, No. 2, pp. 163–169.

Kinetics of Chemical Ionization in Shock Waves: III. Inert Diluent Gas Effect on the Chemical Ionization Rate

Yu. K. Karasevich

Semenov Institute of Chemical Physics, Russian Academy of Sciences, Moscow, 119991 Russia
e-mail: yukarasevich@yandex.ru

Received September 28, 2007

Abstract—An experimental study of ionization in hydrogen azide decomposition and methane oxidation in shock waves is reported. In both cases, the kinetics of chemical ionization changes significantly upon the replacement of argon with helium as the inert diluent gas. The diluent effect is explained in terms of the hypothesis that the reactions responsible for chemical ionization proceed via the formation of an excited intermediate complex. Calculations using kinetic schemes of the ionization processes are carried out.

DOI: 10.1134/S0023158409020013

Chemical ionization, which was discovered in flames [1–3], is an overequilibrium phenomenon. The nonequilibrium nature of ionization was established not only for hydrocarbon flames, but also for some other (ammonia [4, 5], cyanogen [6], etc.) flames and for the relaxation zone behind a strong shock wave in air [7]. This phenomenon is brought about by very exothermic reactions, such as the recombination of atoms or radicals. The formation of strong chemical bonds in these reactions yields an amount of energy close to the ionization potential of the recombination product. These reactions were indeed observed and received the name of associative ionization.

Some authors note the effect of the inert diluent gas on the rate of chemical ionization in various systems. Information concerning this issue is scarce and contradictory. This effect was observed first by Young and John [8]. Studies of chemical ionization in mixtures of nitrogen atoms and oxygen atoms demonstrated that the ionization rate in a helium medium is almost 300 times lower than the ionization rate in argon. The authors only report this fact without providing any explanation. The diluent gas effect on the ionization rate and on the intensity of UV radiation was also studied for the reaction between acetylene and oxygen atoms at room temperature in a helium medium, which was replaced partially or completely with other diluents [9]. It was found that the saturation current changes upon the replacement of helium with another diluent. The efficiency of diluents increases in the order

$$H_2 < He < Ar < N_2 < CO < CF_4 < CO_2.$$

As compared to the ionization rate in helium, the ionization rate in H_2 is 10 times lower and that in CO_2 is 20 times higher. The general scheme of the process suggested in that study allows the observed dependences to be explained qualitatively under certain assumptions, but it suffers from lack of specificity. The diluent gas effect on the sensitivity of the flame-ionization chromatographic detector was studied in [10, 11]. It was observed that the detector current depends on the inert gas added to the gas stream. The efficiency of inert gases was found to increase in the order

$$He < Ne < CO_2 < N_2 < Ar < CO < Kr < Xe \sim CF_4.$$

Note that this order differs significantly from the order reported in [9]. The authors discovered that the efficiency of the diluent increases as its thermal conductivity decreases and made an attempt to explain the observed effect in terms of the temperature difference due to the difference in heat losses. However, in the authors' opinion, the magnitude of the effect appeared to be too high.

The effects of Ar, Ne, N_2, and H_2O on ionization in the acetylene–oxygen flame were studied using a Langmuir probe [12]. It was demonstrated that the introduction of an additive into the flame exerts a marked effect on the total number of electrons in the combustion zone. In order to explain this effect, the authors assumed that the first stage of the associative ionization reaction yields either the excited radical CHO* with an excitation level close to the continuum boundary or the ion CHO^+ and an electron executing finite motion near the ion. The collision of this complex with molecules having a negative electron affinity results in ionization. Colliding with molecules with a positive electron affinity, the complex dissociates into neutral species.

It is clear from the above-quoted works that the diluent gas affects the ionization characteristics of various flames. However, based on these data, it is impossible to make an unambiguous conclusion as to the cause of this effect. All of the above data were obtained for flames, and the ionization kinetics was not studied. There has been a study of the ionization kinetics in the

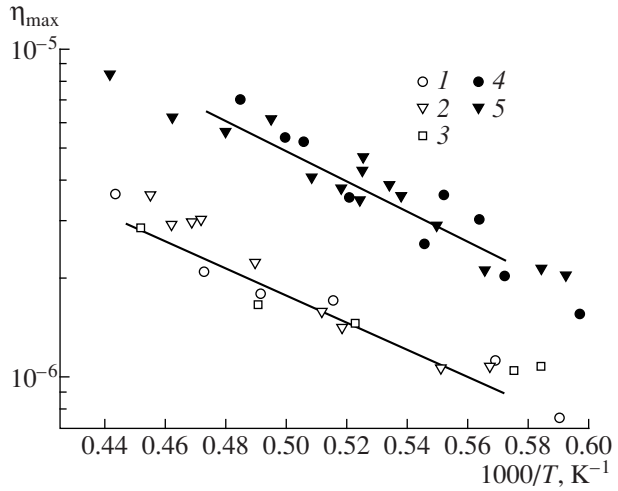

Fig. 1. Temperature dependences of the electron yield in HN_3 decomposition in (*1–3*) argon and (*4*, *5*) helium. HN_3 concentrations: (*1*, *4*) 0.5, (*2*, *5*) 1.0, and (*3*) 2.3%. The points represent experimental data, and the straight lines represent the data calculated using the kinetic scheme (table) for argon and helium.

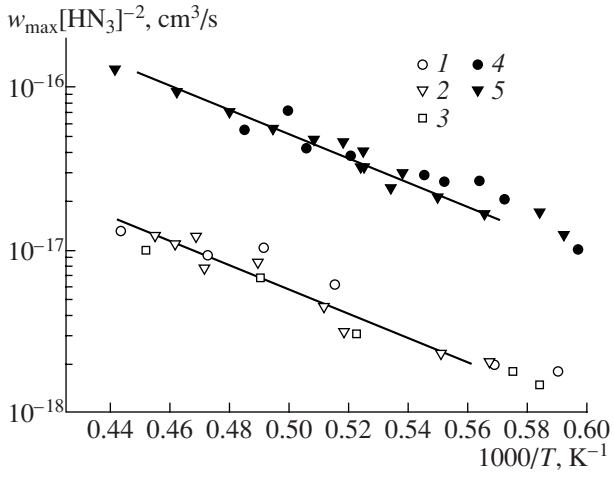

Fig. 2. Temperature dependences of the maximum ionization rate in HN_3 decomposition. The designations are the same as in Fig. 1.

decomposition of hydrogen azide in shock waves under conditions such that there were no problems arising from complicated gas dynamics, transport phenomena, and temperature gradients [13]. It was observed again that the replacement of argon with helium as the diluent gas raises the ionization rate almost by one order of magnitude. For explaining this effect, it was assumed that the associative ionization reaction responsible the ionization process in this system yields an excited intermediate complex.

The study reported here continues the above-cited study [13]. Here, we use more experimental data, including information concerning the effect of the diluent gas on the ionization rate in methane oxidation in shock waves.

EXPERIMENTAL

Measurements were made behind reflected shock waves in the shock tube described in [14]. For hydrogen azide, the temperature range was 1670–2300 K and the pressure range was 0.4–2.3 atm. For methane-containing mixtures, experiments were performed at 2150–3150 K and atmospheric pressure. Thermodynamic parameters of the mixtures behind the reflected shock wave front were derived from incident shock wave velocity data in the one-dimensional shock tube approximation using reference data [15]. The gas temperature and pressure were determined with an error no larger than 1.5 and 5%, respectively. In the experimental study of the ionization kinetics, we used the following mixtures: 0.5, 1.0, or 2.3% HN_3 + argon; 0.5 or 1.0% HN_3 + helium; 0.6% CH_4 + 2.4% O_2 + argon or helium.

We measured the electron concentration as a function of time, $n_e(t)$, and the frequency of collisions between an electron and a species of the surrounding gas using a microwave interferometer with a double-wire line as the probe. Double-wire lines are known to afford a fairly high space resolution of 3–5 mm. The error in the measured electron concentration did not exceed ±30%. A description of the interferometer is presented elsewhere [16]. For hydrogen azide, we additionally measured the intensity of UV radiation from excited NH radicals ($A^3\Pi_u \longrightarrow X^3\Sigma^-$) at a wavelength of $\lambda = 337.5$ nm.

By processing experimental profiles according to the procedure suggested in an earlier work [13], we determined the characteristic parameters of the time dependence of the electron concentration, namely, the maximum ionization rate (w_{max}) and the maximum electron yield per methane or hydrogen azide molecule (η_{max}). For methane-containing mixtures, we additionally determined the induction period (τ_i); for hydrogen azide, the maximum intensity of UV radiation from excited NH radicals ($A^3\Pi_u \longrightarrow X^3\Sigma^-$) at $\lambda =$ 337.5 nm (J_{max}).

RESULTS

Figures 1–6 show the temperature dependences of the parameters characterizing the experimental electron concentration profiles. Initially, we will consider the experimental data obtained for argon as the diluent gas. It is clear from Fig. 1 (data points *1–3*) that the electron yield per reacted HN_3 molecule in argon increases with increasing temperature, and the corresponding activation energy is 19 kcal/mol. At $T = 2250$ K, the electron yield is 3.3×10^{-6}. At the same temperature, the electron yield per carbon atom has a smaller value of 2×10^{-6} (Fig. 4), and the temperature dependence of

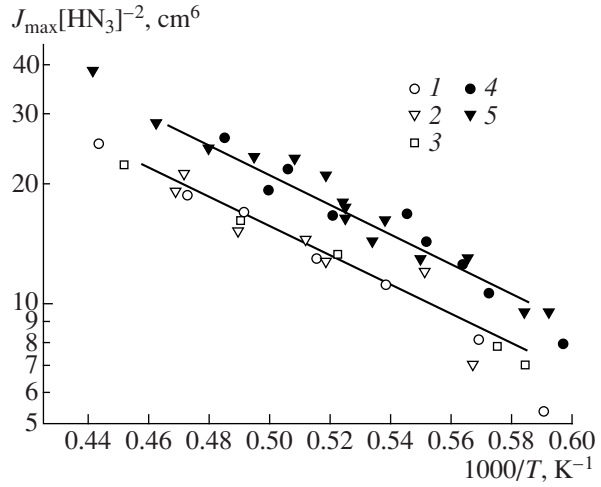

Fig. 3. Temperature dependences of the maximum intensity of radiation from the $NH(A^3\Pi_u)$ radical at $\lambda = 337.5$ nm in HN_3 decomposition. The designations are the same as in Fig. 1.

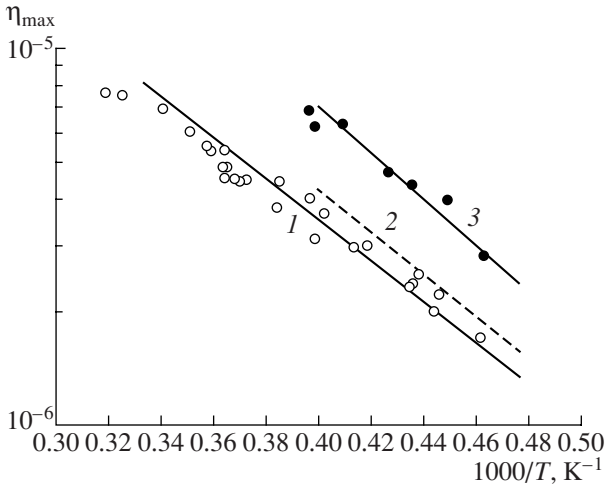

Fig. 4. Temperature dependences of the electron yield in 0.6% CH_4 + 2.4% O_2 mixtures with (*1*) argon and (*2*, *3*) helium. The points represent experimental data; the straight lines represent the data calculated using the kinetic scheme reported in [27] for (*1*) argon, (*2*) helium with $k_{eff}^{Ar} = 1.5 \times 10^{-13}$ cm^3/s, and (*3*) helium with $k_{eff}^{He} = 6.5 \times 10^{-13}$ cm^3/s.

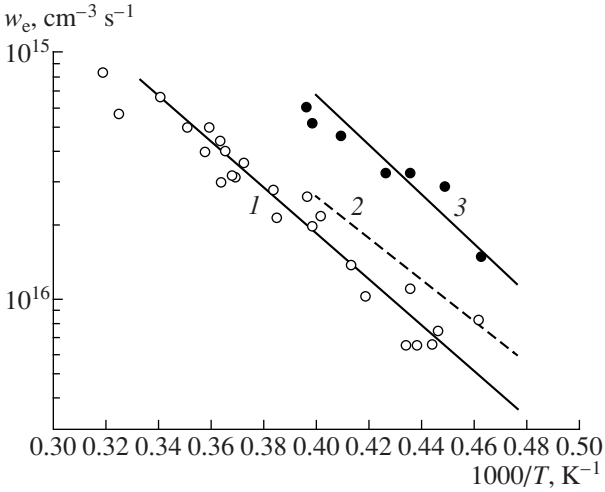

Fig. 5. Temperature dependences of the maximum ionization rate in 0.6% CH_4 + 2.4% O_2 mixtures. The designations are the same as in Fig. 4.

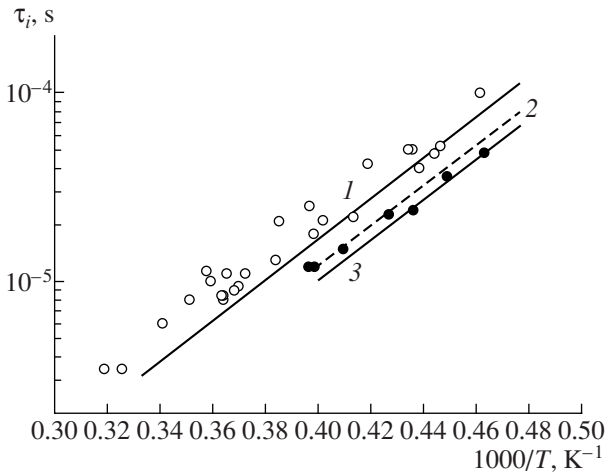

Fig. 6. Temperature dependences of the induction period of ionization in 0.6% CH_4 + 2.4% O_2 mixtures. The designations are the same as in Fig. 4.

the electron yield in this case implies an apparent activation energy of 30 kcal/mol. The ionization rate in HN_3 decomposition is well above the ionization rate in methane oxidation. For example, the maximum ionization rate at 2250 K is 1.7×10^{16} cm^{-3} s^{-1} for the 0.5% HN_3 + Ar mixture (Fig. 2) and 7×10^{14} cm^{-3} s^{-1} for the 0.6% CH_4 + 2.4% O_2 + Ar mixture (Fig. 5, data points *1*). The ionization process in HN_3 decomposition begins immediately after the arrival of the reflected shock wave front at the measurement cross section. In methane oxidation, ionization takes place after some time delay (Fig. 6, data points *1*). Note that the ionization rate in HN_3 decomposition peaks at nearly the same time as the intensity of radiation from excited NH radicals ($A^3\Pi_u \longrightarrow X^3\Sigma^-$). Figure 2 (data points *1–3*) presents the temperature dependence of the $w_{max}/[HN_3]^2$ ratio observed for argon-diluted mixtures. This ratio best characterizes the observed dependence of the ionization rate on the hydrogen azide concentration in the initial mixture. Similar behavior is shown by the temperature dependence of the $J_{max}/[HN_3]^2$ ratio (Fig. 3).

The replacement of argon with helium changes all of the parameters considered, as is clearly demonstrated in Figs. 1–6. The electron yield from HN_3 decomposition in the helium-diluted mixtures is ~2.5 times higher than the electron yield observed for the argon-diluted mixtures (Fig. 1). In the case of methane oxidation, the replacement of argon with helium raises the electron yield by a factor of ~1.8 (Fig. 4). The ionization rate in HN_3 decomposition increases by nearly one order of magnitude (Fig. 2), while the radiation intensity increases by a much smaller factor of 1.3 (Fig. 3). An increase in the ionization rate upon the replacement of argon with helium is also observed for methane oxidation, but this effect is somewhat weaker than in the case of HN_3 decomposition: the ionization rate increases by a smaller factor of 3.5 (Fig. 5). This is accompanied by a shortening of the induction period of ionization (Fig. 6).

DISCUSSION

Let us first consider the diluent effect on ionization in HN_3 decomposition. An earlier analysis of experimental data for this process [13] provided strong evidence in favor of the ionization and excitation mechanism based on the following reactions:

$$HN_3 + M \longrightarrow NH(a^1\Delta) + N_2 + M, \quad \text{(I)}$$

$$NH(a^1\Delta) + NH(a^1\Delta) \longrightarrow N_2H_2^+ + e^-, \quad \text{(II)}$$

$$NH(a^1\Delta) + NH(a^1\Delta) \longrightarrow NH(A^3\Pi_u) + NH(X^3\Sigma^-). \quad \text{(III)}$$

It was demonstrated earlier that HN_3 decomposition in shock waves (reaction (I)) above 1200 K proceeds via a spin-allowed channel, yielding the singlet electronically excited radical $NH(a^1\Delta)$ [17].

In a previous work [13], we presented qualitative considerations suggesting that the marked effect of the inert gas diluent on the ionization rate is due to reaction (II) proceeding via the formation of the intermediate excited complex $N_2H_2^*$. Let us consider this phenomenon in greater detail.

Obviously, the diluent gas effect on the ionization rate can be due to the change in the concentration of reacting $NH(a^1\Delta)$ radicals that arises from changes in their formation and disappearance rates or to the direct participation of diluent molecules in reaction (II). Since the electronically excited radical $NH(a^1\Delta)$ is involved in reaction (II), there is good reason to assume that the effect of the diluent is due to the fact that argon and helium quench the excited state with different efficiencies. At first glance, the observed effect is in qualitative agreement with these considerations. Suppose that the disappearance of the $NH(a^1\Delta)$ radical is mainly due to the quenching of excitation via the collision of this radical with an atom of the diluent:

$$NH(a^1\Delta) + M \longrightarrow NH(X^3\Sigma^-) + M. \quad \text{(IV)}$$

By consideration of the two consecutive reactions (I) and (IV), we obtained an analytical expression for the concentration of $NH(a^1\Delta)$ radicals as a function of time. From this expression, we found that the integrated electron yield in reaction (II) is

$$\eta_i = \frac{k_2}{[HN_3]}\int_0^\infty [HN(a^1\Delta)]^2 dt = \frac{1}{2}\frac{[HN_3]}{[M]}\frac{k_2}{k_1}\frac{\kappa^2}{1+\kappa}, \quad (1)$$

where $\kappa = k_1/k_4$.

It follows from relationship (1) that the electron yield must be inversely proportional to the gas pressure and proportional to the initial HN_3 concentration. In fact, no dependence of the electron yield on the initial HN_3 concentration or pressure was observed in our experiments (Fig. 1). Furthermore, the $NH(a^1\Delta)$ disappearance rate in HN_3 photolysis in argon depends only on the HN_3 concentration even when it is as low as 0.1% [18], indicating that the electronic excitation of $NH(a^1\Delta)$ is quenched only weakly by processes involving argon.

This analysis demonstrates that the reactions involving the diluent in argon and helium either make approximately equal contributions to the formation of the $NH(a^1\Delta)$ concentration profile or, more likely, are insignificant. Therefore, the effect of the diluent gas on the formation and disappearance of $NH(a^1\Delta)$ radicals cannot account for the changes in the ionization rate caused by the replacement of one diluent by the other.

For this reason, in order to explain the observed difference between the ionization rates, we will assume that the diluent is directly involved in reaction (II). If this is the case, the reaction will proceed via the formation of an intermediate complex, specifically, the excited radical $N_2H_2^*$ with an excitation level close to the continuum boundary or the ion $N_2H_2^+$ and an electron executing finite motion near this ion, just as was assumed in [12].

Consider the following scheme of the associative ionization of species A and B through the formation of the electron-excited intermediate complex AB*:

$$\begin{aligned} &\text{(a) } A + B \underset{\gamma_{-a}}{\overset{\gamma_a}{\rightleftarrows}} AB^*, \\ &\text{(b) } AB^* \xrightarrow{\gamma_b} AB^{r\nu}, \\ &\text{(c) } AB^* + M \xrightarrow{\gamma_c} \text{products}, \\ &\text{(d) } AB^* + M \xrightarrow{\gamma_d} AB^+ + e^-. \end{aligned} \quad \text{(V)}$$

In scheme (V), reaction (a) describes the collisional formation of the complex and its spontaneous decomposition into the initial reactants; reaction (b) is the deactivation of the complex by the conversion of its electronic excitation into the vibrational–rotational excitation of AB; reactions (c) and (d) describe, respectively, the deactivation and ionization of the complex upon its collision with a particle of the surrounding gas.

In the quasi-steady-state approximation for the AB* concentration, we obtain the following expression for the ionization rate:

$$w_e = [A][B]\frac{\gamma_a\gamma_d}{\gamma_b + \gamma_{-a}}\frac{[M]}{1 + \frac{\gamma_c + \gamma_d}{\gamma_b + \gamma_{-a}}[M]}. \quad (2)$$

In the high-pressure limit, when

$$G = \frac{\gamma_c + \gamma_d}{\gamma_b + \gamma_{-a}}[M] \gg 1, \quad (3)$$

the ionization rate appears as

$$w_e = [A][B]\frac{\gamma_a\gamma_d}{\gamma_b + \gamma_d} = k_{eff}[A][B]; \quad (4)$$

for $G \ll 1$,

$$w_e = [A][B]\frac{\gamma_a\gamma_d}{\gamma_b + \gamma_{-a}} = k_{eff}[A][B][M]. \quad (5)$$

Since no pressure dependence of the ionization rate was observed in our experiments (Fig. 2), it should be accepted that the case of high pressures (expression (4)) actually takes place. Accordingly, the effect of diluent gas replacement is due to the fact that the ratio of the rate constant of ionization (Vd) to the rate constant of deactivation (Vc) takes different values for collisions of the complex with different particles.

It can be assumed that the intermediate complex has the structure of the so-called Rydberg state, in which the entire excitation energy is accumulated in one of the electrons. There are indications that the Rydberg state plays a significant role in recombination [19] (opposite to ionization), including dissociative recombination [20] (opposite to associative ionization).

The excitation energy of the outer electron of a Rydberg molecule is close to the ionization potential, and, therefore, this electron has a low kinetic energy (<1 eV). Owing to the Ramsauer effect, argon has an anomalously small electron scattering cross section at low collision energies (~1 eV). The Ramsauer effect in helium is not pronounced.

The difference between the electron scattering cross sections of argon and helium was clear in our experiments. The frequency of collisions between electrons and surrounding gas species at atmospheric pressure, measured with a microwave interferometer, is $\nu_{Ar} = (1.5 \pm 0.4) \times 10^{10}$ s^{-1} for argon and has a larger value of $\nu_{He} = (8 \pm 3) \times 10^{10}$ s^{-1} for helium. The scattering cross sections estimated from these measurements are $\sigma_{Ar} = (6.1 \pm 1.5) \times 10^{-16}$ cm^2 for argon and $\sigma_{He} = (3.3 \pm 1.3) \times 10^{-15}$ cm^2 for helium. If both reaction (Vc) and reaction (Vd) occur via the scattering of the outer electron of the excited transition complex on atoms of the surrounding gas, it is possible to estimate the total values of their rate constant in different gases:

in argon,

$$(\gamma_c + \gamma_d)_{Ar} = 2.4 \times 10^{-11} \text{ cm}^3/\text{s}; \quad (6a)$$

in helium,

$$(\gamma_c + \gamma_d)_{He} = 2.9 \times 10^{-10} \text{ cm}^3/\text{s}. \quad (6b)$$

The above analysis provided a qualitative understanding of the ionization mechanism in HN_3 decomposition. Based on this understanding, neglecting the insignificant effects of the reactions involving secondary decomposition products at high temperatures, it is possible to construct a comparatively simple kinetic model for excitation and ionization by limiting the consideration to the minimum of the $NH(a^1\Delta)$ formation and disappearance reactions above 1700 K. As the temperature is decreased below 1700 K, the reactions involving secondary decomposition products play a progressively more significant role, greatly complicating the overall process.

The corresponding kinetic scheme is presented in the table, which lists preexponential factors for argon and helium (A, cm^3/s; for reaction no. 9, s^{-1}) and activation energies (E, kcal/mol) defined as $k = A_{exp}(-E/RT)$.

This kinetic model is not considered to be complete. The rate constant of reaction no. 1 (HN_3 decomposition) was obtained by extrapolation of lower temperature data [17] (for helium, the constant was multiplied by a factor of 2.5 [21]), and the rate constant of reaction no. 2 was taken from [22]. The rate constants of the other reactions included in the table were fitted to the experimental electron concentration and radiation intensity profiles and their temperature dependences. It is accepted that the radiation intensity is proportional to the rate of reaction no. 14. An analysis of the dependences of the ionization parameters for HN_3 decomposition on the gas pressure and on the concentration of the initial compound led us to conclude that associative ionization takes place via mechanism (V) at high temperatures ($G \gg 1$). The lifetime of the electronically excited intermediate complex $N_2H_2^*$ is $\tau^* = 1/k_7 \approx 0.3$ μs. Shortening this time by one order of magnitude brings the criterion G to a value of ~ 1. This means that the complex should have a rather long lifetime. There is evidence that the Rydberg states of molecules can be fairly stable in some cases [23–26]. With the rate constants of reaction nos. 8 and 9 obtained under the assumption that relationships (6) are valid, the ionization process takes place in the high-pressure regime ($G \gg 1$). The effective ionization rate constant determined from Eq. (4) is $k_{eff}^{Ar} = 87 \times 10^{-14}\exp(-E_5/RT)$ cm^3/s for argon and $k_{eff}^{He} = 3.5 \times 10^{-13}\exp(-E_5/RT)$ cm^3/s for helium, where $E_5 = 30$ kcal/mol is the activation energy of reaction no. 5.

The corresponding set of equations was solved numerically for the following conditions: $T = 1750$–2250 K, $P = 0.5$–2.5 atm, and initial HN_3 concentrations of 0.5–2.5%. Good agreement with experimental data (points) was attained for the calculated tempera-

Kinetic model of ionization and excitation in HN_3^* decomposition

No.	Reaction	A, cm^3/s		E, kcal/mol
		argon	helium	
1	$HN_3 + M \longrightarrow NH(a^1\Delta) + N_2 + M$	3.2×10^{-9}	8.0×10^{-9}	40
2	$HN_3 + NH(a^1\Delta) \longrightarrow$ products	9.0×10^{-13}		0
3	$NH(a^1\Delta) + M \longrightarrow NH(X^3\Sigma^-) + M$	5.0×10^{-15}	4.0×10^{-15}	0
4	$NH(a^1\Delta) + NH(a^1\Delta) \longrightarrow$ products	8.0×10^{-12}		0
5	$NH(a^1\Delta) + NH(a^1\Delta) \longrightarrow N_2H_2^*$	3.0×10^{-12}		30
6	$N_2H_2^* \longrightarrow NH(a^1\Delta) + NH(a^1\Delta)$	3.0×10^{4}		0
7	$N_2H_2^* \longrightarrow$ products	3.0×10^{6}		0
8	$N_2H_2^* + M \longrightarrow$ products + M	2.3×10^{-11}	2.5×10^{-10}	0
9	$N_2H_2^* + M \longrightarrow N_2H_2^+ + e^- + M$	7.0×10^{-13}**	3.3×10^{-11}**	0
10	$N_2H_2^+ + e^- \longrightarrow$ products	2.0×10^{-7}		0
11	$2NH(a^1\Delta) \longrightarrow NH(A^3\Pi_u) + NH(X^3\Sigma^-)$	3.5×10^{-14}		11.5
12	$NH(A^3\Pi_u) \longrightarrow NH(X^3\Sigma^-)$	1.0×10^{5}		0
13	$NH(A^3\Pi_u) + M \longrightarrow NH(X^3\Sigma^-) + M$	5.0×10^{-14}	4.0×10^{-14}	0
14	$NH(A^3\Pi_u) + M \longrightarrow NH(X^3\Sigma^-) + M + h\nu$	1.0×10^{-15}	1.5×10^{-15}	0

* The rate constant is represented as $k = A\exp(-E/kT)$.
** The dimension of A for reaction no. 9 is s^{-1}.

ture dependences of η_{max} and w_{max} (straight lines in Figs. 1 and 2). Because of the relativeness of the radiation intensity measurements, the calculation was locked on experimental data so that the maximum values of the calculated and observed radiation intensity were equal for the 0.5% HN_3 + Ar mixture at T = 1850 K. In the other calculations, the resulting conversion factor between the calculated rate of reaction no. 13 and the radiation intensity was the same. The solid lines in Fig. 3 represent calculated temperature dependences of J_{max}. As the initial HN_3 concentration and the pressure were varied by a factor of 5, the calculated temperature dependences of the ionization profile parameters differed by at most 25%. Figures 1–3 plot the dependences averaged over all calculations.

Thus, although the kinetic model in question is approximate, it provides a good description for the ionization and excitation kinetics in hydrogen azide decomposition in argon and helium media.

The formation of ionized products in hydrocarbon combustion is due to the associative ionization reaction

$$CH + O \longrightarrow CHO^+ + e^-. \qquad \text{(VI)}$$

As distinct from the radical $NH(a^1\Delta)$, which appears in the first step of HN_3 decomposition, the radical CH results from a long sequence of reactions. The kinetic scheme of ionization in methane combustion [27], which is based on the methane combustion mechanism [28], contains tens of reactions involving particles of the diluent gas. The scheme is in good agreement with experimental kinetic data for the ionization of methane–oxygen mixtures in argon (Figs. 4–6).

We will use the scheme suggested in [27] to evaluate the effect of the diluent gas on the parameters of ionization according to reaction (VI). However, the literature contains no rate constant data for reactions involving diluent gas particles in helium. For this reason, we will assume that the rate constants of all of these reactions change in proportion to the change in the collision frequency upon the replacement of argon with helium. Accordingly, the rate constants increase by a factor of 2–2.5. The ionization parameters calculated using this change of rate constants are plotted in Figs. 4–6 (curves *2*). It can be seen in Fig. 6 that the change in the calculated induction period of ionization is nearly equal to the observed change. At the same time, although the calculated temperature-dependent maximum electron yield (Fig. 4) and maximum ionization rate (Fig. 5) increase, the calculated changes are smaller than the observed changes. Firstly, this result suggests that the above change of the rate constants accounts correctly for the changes occurring in methane oxidation upon the replacement of argon with helium, because the calculated and observed changes in the characteristic times are equal. Secondly, it can be assumed that reaction (VI) yields the electronically excited intermediate complex CHO*, similarly to reaction (II). The effective

rate constant of reaction (VI) will then be $k_{\text{eff}}^{\text{Ar}} = 1.5 \times 10^{-13}$ cm^3/s for argon (as in [27]) and $k_{\text{eff}}^{\text{He}} = 6.5 \times 10^{-13}$ cm^3/s for helium. The temperature dependences of the ionization parameters calculated in terms of the kinetic scheme presented in [27] with the rate constant $k_{\text{eff}}^{\text{He}}$ are shown in Figs. 4–6 (curves *3*).

CONCLUSIONS

We have considered two examples illustrating the dependences of the chemical ionization kinetics in shock waves on the nature of the inert diluent gas. In both cases, we were able to simulate this phenomenon quantitatively under the assumption that the associative ionization reactions responsible for ionization yield an excited intermediate complex. Since it was possible to describe two different associative ionization reactions in unified terms, it can be assumed that the formation of the excited intermediate complex is a common feature of associative ionization reactions. However, in order to verify this hypothesis, it is necessary to understand the physical mechanism responsible for the fact that the electron during the reaction is mainly in the bound, not free, state. In addition, there is a macrokinetic effect because of the difference between the complex ionization and complex deactivation rate constant ratios in collisions with different species. In order to find out the cause of these differences, it is necessary to study the dynamics of these collisions.

REFERENCES

1. Aravin, G.S., *Cand. Sci. (Phys.–Math.) Dissertation*, Moscow: Inst. Chem. Phys., 1951.
2. Calcott, H.F., *3 Symp. (Int.) on Combustion*, 1949, p. 245.
3. Miller, M.J., *14th Symp. (Int.) on Combustion*, 1973, p. 307.
4. Peeters, J. and Vinckier, C., *15th Symp. (Int.) on Combustion*, 1974, p. 969.
5. Bertrand, C. and van Tiggelen, P.J., *J. Phys. Chem.*, 1974, vol. 78, p. 2320.
6. Bulewicz, E.M. and Padley, P.J., *9 Symp. (Int.) on Combustion*, 1963, p. 647.
7. Lin, S.C. and Tear, J.D., *Phys. Fluids*, 1963, vol. 6, p. 355.
8. Young, R.A. and John, G.St., *J. Chem. Phys.*, 1966, vol. 45, p. 4156.
9. Blades, A.T., *J. Chromatogr. Sci.*, 1976, vol. 14, p. 45.
10. Chawner, B.L. and Blades, A.T., *Can. J. Chem.*, 1978, vol. 56, p. 2273.
11. Chawner, B.L. and Blades, A.T., *Can. J. Chem.*, 1978, vol. 56, p. 2278.
12. Zaitsev, A.S., Tverdokhlebov, V.I., and Tverdokhlebova, L.S., *Teplofiz. Vys. Temp.*, 1980, vol. 18, no. 3, p. 634.
13. Aravin, G.S., Karasevich, Yu.K., and Vlasov, P.A., *Khim. Fiz.*, 1982, vol. 1, no. l0, p. 1360.
14. Aravin, G.S., Karasevich, Yu.K., and Shumeiko, A.N., *Fiz. Goreniya Vzryva*, 1977, no. 5, p. 721.
15. *Termodinamicheskie svoistva individual'nykh veshchestv: Spravochnik* (Thermodynamic Properties of Individual Substances), Glushko, V.P., Ed., Moscow: Akad. Nauk SSSR, 1962.
16. Vlasov, P.A., Karasevich, Yu.K., and Smirnov, V.N., *Teplofiz. Vys. Temp.*, 1997, vol. 35, no. 2, p. 200 [*High Temp.* (Engl. Transl.), vol. 35, no. 2, p. 198].
17. Demin, A.I., Zaslonko, I.S., Kogarko, S.M., and Mozzhukhin, E.V., *Kinet. Katal.*, 1973, vol. 14, p. 283.
18. Paur, R.J. and Bair, E.J., *J. Photochem.*, 1973, no. 1, p. 255.
19. Zhdanov, V.P., *J. Phys. B*, 1980, vol. 13, p. L311.
20. Kupriyanov, S.E., *Zh. Eksp. Teor. Fiz.*, 1965, vol. 48, p. 467.
21. Zaslonko, I.S., Kogarko, S.M., and Mozzhukhin, E.V., *Fiz. Goreniya Vzryva*, 1976, no. 1, p. 4.
22. Okabe, H., *J. Chem. Phys.*, 1968, vol. 49, no. 6, p. 2726.
23. Delpech, J.-F., *XV Int. Conf. on Phenomena in Ionized Gases*, Minsk, 1981, p. 131.
24. Yang, R.A., *Int. J. Chem. Kinet.*, 1982, vol. 14, no. 2, p. 93.
25. Herzberg, G., *Faraday Discuss. Chem. Soc.*, 1981, vol. 71, p. 165.
26. King, H.F. and Morokuma, K., *J. Chem. Phys.*, 1979, vol. 71, p. 3213.
27. Karasevich, Yu.K., *Kinet. Katal.*, 2009, vol. 50, no. 1, p. 80.
28. Tereza, A.M., Slutskii, V.G., and Severin, E.S., *Khim. Fiz.*, 2003, vol. 22, no. 6, p. 30.